

Article

Cytospyrone and Cytospomarin: Two New Polyketides Isolated from Mangrove Endophytic Fungus, *Cytospora* sp.[†]

Chengwen Wei¹, Qin Deng², Mengyu Sun¹ and Jing Xu^{1,2,*}

¹ Key Laboratory of Advanced Materials of Tropical Island Resources of Ministry of Education, School of Chemical Engineering and Technology, Hainan University, Haikou 570228, China; chengwen121412@163.com (C.W.); sunmengyu0305@163.com (M.S.)

² College of Horticulture and Landscape, Hainan University, Haikou 570228, China; dengqin_e@yeah.net

* Correspondence: happyjing3@hainanu.edu.cn; Tel.: +86-898-6627-9226; Fax: +86-898-6627-9010

† Dedicated to Prof. Dr. Peter Proksch on His Research Career in Marine Natural Product Chemistry.

Academic Editor: Akihito Yokosuka

Received: 24 August 2020; Accepted: 10 September 2020; Published: 15 September 2020



Abstract: Two new polyketides, cytospyrone (1), cytospomarin (2), together with three known metabolites dimethoxyphtalide (3), integracin A (4) and integracin B (5), were isolated from the culture of *Cytospora* sp. from the Chinese mangrove *Ceriops tagal*. Their structures were elucidated by extensive spectroscopic analyses and time dependent density functional theory (TDDFT), calculation of electronic circular dichroism (ECD) and optical rotation (OR) data. Compound 2 displayed weak inhibitory activity against *Escherichia coli* GIM1.201 (minimum inhibitory concentration (MIC) value of 0.35 mM). Compounds 4 and 5 displayed significant cytotoxicity against human cancer cell line HepG2 (IC₅₀ values of 5.98 ± 0.12 μM and 9.97 ± 0.06 μM, respectively), more potent than the positive control 5-fluorouracil (IC₅₀ value of 43.50 ± 3.69 μM).

Keywords: *Cytospora* sp.; polyketides; structure identification; antimicrobial activity; cytotoxicity

1. Introduction

Mangrove endophytic fungi are attracting considerable attention from natural product chemists and biologists alike and a great deal of structurally diverse natural products with unusual biological activity have been discovered recently [1–3]. Fungal genera *Alternaria*, *Aspergillus*, *Cladosporium*, *Colletotrichum*, *Fusarium*, *Paecilomyces*, *Penicillium*, *Pestalotiopsis*, *Phoma*, *Phomopsis*, *Phyllosticta*, and *Trichoderma* are considered as the predominant producer of the most notable bioactive secondary metabolites [4–6]. However, due to the high rediscovery of previously known compounds and scaffolds from these well-investigated organisms, neglected fungal species that are poorly studied might be an alternative source for the discovery of new bioactive compounds.

During our ongoing screening for biologically active secondary metabolites from mangrove endophytic fungi [7–10], we recently investigated *Cytospora* sp., an endophytic fungus derived from the hypocotyls of Chinese mangrove *Ceriops tagal*, resulting in the isolation of a new antimicrobial bicyclic sesquiterpene, seiricardine D, together with eight known metabolites [11]. Further study of the aforementioned *Cytospora* sp. afforded two new polyketides, cytospyrone (1), cytospomarin (2), together with three known metabolites dimethoxyphtalide (3) [12], integracin A (4) [13], and integracin B (5) (Figure 1) [13].

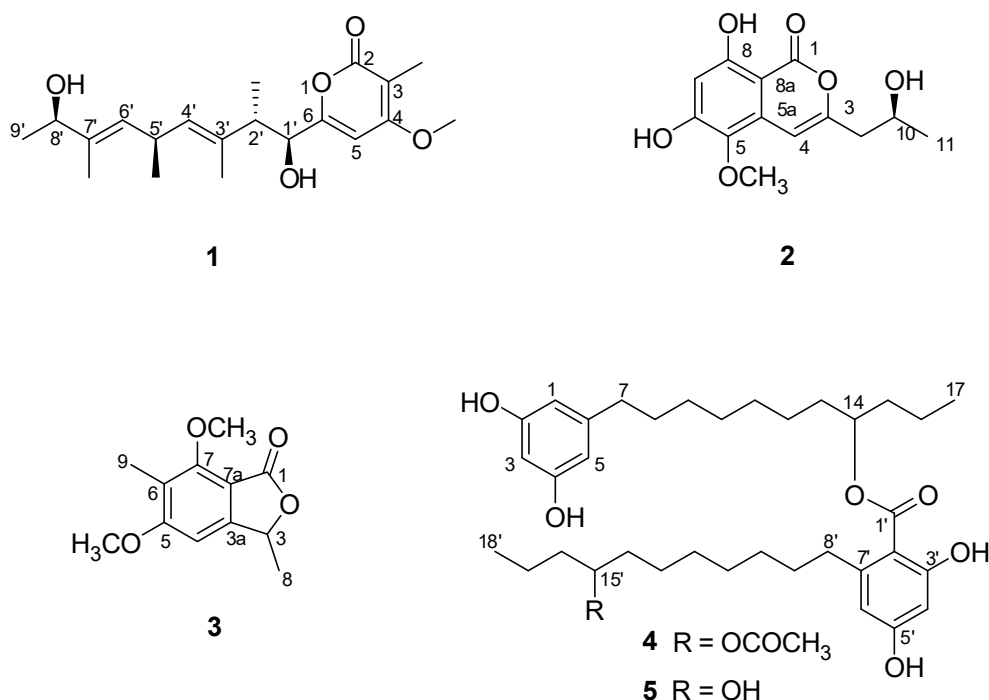


Figure 1. Structures of compounds 1–5.

2. Results and Discussion

2.1. Isolation and Structure Elucidation

Cytospyrone A (**1**) was isolated as a white amorphous powder, and has the molecular formula $C_{20}H_{30}O_5$ established by high resolution electrospray ionization mass spectroscopy (HR-ESI-MS) at m/z 373.1988 $[M + Na]^+$ (calculated for 373.1991), indicating six degrees of unsaturation. The 1H and ^{13}C nuclear magnetic resonance (NMR) data of **1** in association with distortionless enhancement by polarization transfer (DEPT) and heteronuclear single quantum coherence (HSQC) spectrum suggested the presence of six upfield methyls [δ_H 1.03, (d, $J = 6.7$), δ_C 21.7, q, 5'-CH₃; 1.07, (d, $J = 7.0$), δ_C 16.2, q, 2'-CH₃; 1.18, (d, $J = 6.4$), δ_C 21.9, q, 9'-CH₃; 1.65, s, δ_C 11.8, q, 7'-CH₃; 1.67, s, δ_C 10.9, q, 3'-CH₃; 1.85, s, δ_C 8.4, q, 2'-CH₃], a methoxy group (δ_H 3.94, s, δ_C 57.3, q, 4-OCH₃), three olefinic signals [δ_H 5.26, (d, $J = 9.0$), δ_C 130.0, d, CH-6'; δ_H 5.32, (d, $J = 9.1$), δ_C 130.0, d, CH-4'; δ_H 6.47, s, δ_C 97.5, d, CH-5], four methines [2.79, m, δ_C 44.1, d, 2'-CH; 3.33–3.42, m, δ_C 32.3, d, 5'-CH; 4.08, (d, $J = 9.6$), δ_C 80.7, d, 1'-CH; 4.10, (q, $J = 6.4$), δ_C 73.9, d, 8'-CH], and six quaternary carbons (δ_C 101.5, 134.2, 138.1, 167.8, 168.5, 169.1). Two substructures, an α -pyrone moiety and a linear aliphatic chain, were assigned by analyses of detailed interpretation of 1H - 1H correlation spectroscopy (COSY) and heteronuclear multiple bond correlation (HMBC) correlations (Figure 2). The α -pyrone moiety was established by HMBC correlations from 3-CH₃ to carbons C-2, C-3 and C-4, and from H-5 to C-4 and C-6. Presence of the methoxy group at C-4 was corroborated from the HMBC correlation of its protons (δ_H 3.94, s) with C-4 (δ_C 169.1) and nuclear overhauser effect spectroscopy (NOESY) correlations between 3-CH₃/4-OCH₃ and H-5/4-OCH₃. A linear aliphatic chain with a thirteen carbon unit was determined by the interpretation of 1H - 1H COSY and HMBC spectroscopic data. The COSY cross-peaks [H-1'/H-2'/2'-CH₃, H-3'/H-4'/4'-CH₃/H-5', H-8'/H-9'] and HMBC correlations from 2'-CH₃ to carbons C-1', C-3', from 3'-CH₃ to carbons C-2', C-3' and C-4', from 7'-CH₃ to carbons C-6', C-7' and C-8', and from H-9' to C-7' permitted the construction of a linear aliphatic chain. The above two structural fragments were finally connected to construct the planar structure of compound **1** from the key HMBC correlations from H-1' and H-2' to C-6, from H-5 to C-2'. The relative configuration of **1** was deduced by analysis of the NOESY data. The NOESY correlations (Figure 3) between H-1'/2'-CH₃, 2'-CH₃/H-4', H-2'/3'-CH₃, H-4'/H-5', H-5'/H-6', 7'-CH₃/H-8' and H-6'/H-8'

suggested that they were positioned on the same face and both Δ^4 and Δ^6 double bonds were assigned to the *E*-configuration. In addition, the correlations of H-1'/3'-CH₃, 3'-CH₃/5'-CH₃ and 5'-CH₃/7'-CH₃ revealed they were positioned on the other face. To define its absolute configuration, the time dependent density functional theory—(TDDFT)-calculated electronic circular dichroism (ECD) spectrum at the B3LYP/6-31+g (d, p) level was compared with the experimental circular dichroism (CD) spectrum (Figure 4). Therefore, the structure of **1** was established as 6-((1*S*, 2*S*, 3*E*, 5*R*, 6*E*, 8*R*)-1,8-dihydroxy-2,3,5,7-tetramethylnona-3,6-dienyl)-4-methoxy-3-methyl-2*H*-pyran-2-one.

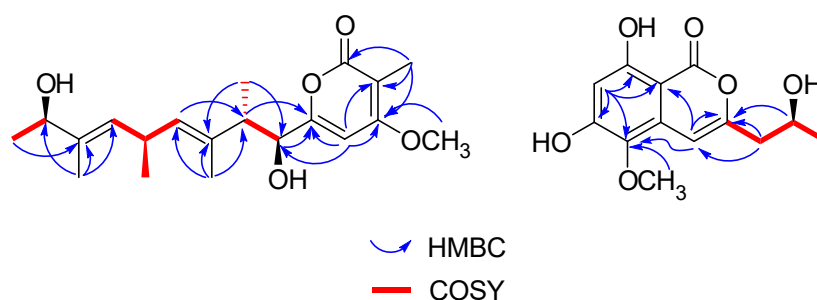


Figure 2. Key HMBC, ¹H-¹H COSY correlations of **1** and **2**.

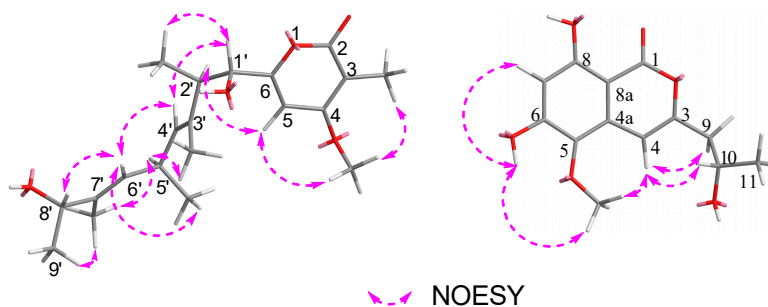


Figure 3. Key NOESY correlations of **1** and **2**.

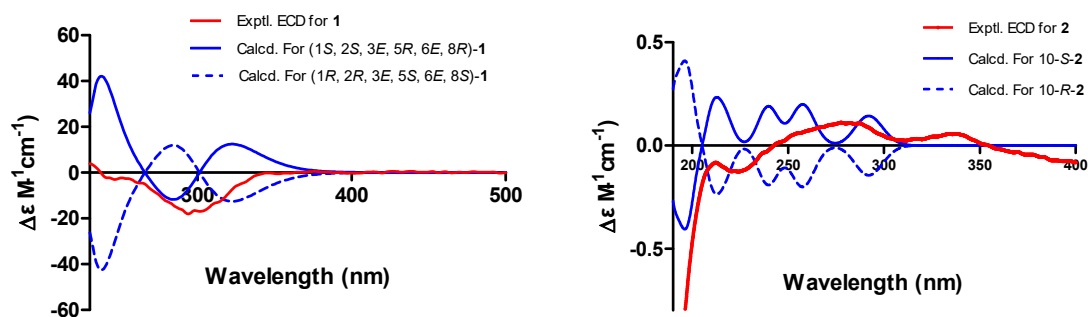


Figure 4. Experimental and calculated electronic circular dichroism (ECD) spectra of **1** and **2**.

Cytospomarin (**2**), a yellow amorphous solid, was found to have the molecular formula C₁₃H₁₄O₆, established by HR-ESI-MS (*m/z* 289.0674, calculated for [M + Na]⁺ 289.0688), implying seven degrees of unsaturation. The ¹H and ¹³C NMR data of **2** indicated that six of the seven units of unsaturation could be due to an aromatic ring, a double bond, and one carbonyl group. Thus, the remaining unit of unsaturation was attributed to a ring formation. The ultraviolet (UV) absorption maxima at 247 and 318 nm suggested **2** is an isocoumarin derivative. The ¹H and ¹³C NMR data of **2** and the DEPT and HSQC spectra revealed the presence of two methyl groups, including a methoxy group (δ_{H} 3.68, s, δ_{C} 60.4, q, 5-OCH₃) and a terminal alkyl methyl [δ_{H} 1.12, (d, *J* = 6.2), δ_{C} 23.3, q, 11-CH₃], a methylene (δ_{H} 2.50–2.57, m, δ_{C} 42.8, t, CH₂-9), two olefinic methines [δ_{H} 6.33, s, δ_{C} 102.6, d, CH-7; δ_{H} 6.53, s, δ_{C} 99.9, d, CH-4], an oxymethine (δ_{H} 3.92–4.00, m, δ_{C} 64.0, d, CH-10) and seven quaternary carbons, including a carbonyl (δ_{C} 165.6, s, C-1). The ¹H and ¹³C NMR and HSQC

spectra of compound **2** closely resembled those of an isocoumarin compound peniisocoumarin G [14], recently isolated from another endophytic fungus, *Penicillium commune* QQF-3, obtained from fresh fruit of the mangrove plant *Kandelia candel*, indicating that **2** might have the same basic molecular framework as peniisocoumarin G. The only difference between these was replacement of the hydroxyl substituent of peniisocoumarin G by a methoxy group in **2**. The HMBC and NOESY correlations (Figures 2 and 3) supported the assignments of the methoxy group 5-OCH₃ (δ_{H} 3.68, s) at C-5 (δ_{C} 134.3). The configuration of C-10 was determined by comparison of optical rotation with the known compounds peniisocoumarin G [14] and botryosphaerin A [15]. The result indicated that compound **2** has the same positive value as those two isocoumarins. It was confirmed by comparing experimental and calculating ECD spectra and optical rotation ($[\alpha]_{\text{D}}^{20} = +11.7^{\circ}$ (c 0.3, MeOH); calculated for $[\alpha]_{\text{D}}^{20} = +89.6^{\circ}$ (MeOH)) of **2** using TDDFT (Figure 4). Accordingly, compound **2** was determined as (S)-6,8-dihydroxy-3-(2-hydroxypropyl)-5-methoxy-1H-isochromen-1-one and named as cytospomarin.

2.2. Bioactivities

Compounds **1–5** were testing the in vitro antimicrobial activity against four human pathogens *Escherichia coli* GIM1.201, methicillin-resistant *Staphylococcus aureus* GIM1.771 (MRSA), *Pseudomonas aeruginosa* GIM1.200, *Candida albicans* GIM2.169, together with three plant pathogens including *Bacillus subtilis*, *Colletotrichum gloeosporioides* and *Magnaporthe oryzae*, and the results are summarized in Table 1. Compound **1–5** were also tested in vitro against the human cancer cell line HepG2 with 5-fluorouracil as the positive control. Among them, compound **2** exhibited weak inhibitory activity against *E. coli* GIM1.201 (minimum inhibitory concentration (MIC) = 0.35 mM) and *M. oryzae* (MIC = 1.41 mM). Compounds **4** and **5** displayed significant cytotoxicity against human cancer cell line HepG2 with IC₅₀ values of $5.98 \pm 0.12 \mu\text{M}$ and $9.97 \pm 0.06 \mu\text{M}$, respectively, more potent than the positive control 5-fluorouracil (IC₅₀ = $43.50 \pm 3.69 \mu\text{M}$) (Table 2).

Table 1. Antimicrobial activities of compounds **1–5**.

Compound	MIC (mM)						
	<i>E. coli</i> GIM1.201	MRSA GIM1.771	<i>P. aeruginosa</i> GIM1.200	<i>C. albicans</i> GIM2.169	<i>B. subtilis</i>	<i>C. gloeosporioides</i>	<i>M. oryzae</i>
1	-	-	-	-	-	-	-
2	0.35	-	-	-	-	-	1.41
3	-	1.94	-	-	-	-	-
4	-	-	-	-	-	-	-
5	-	-	-	-	-	-	-
amphotericin	-	-	-	45.7 μM	-	7.6 μM	7.6 μM
ciprofloxacin	0.07	0.14	0.07	-	0.14	-	-

-: not detectable.

Table 2. Cytotoxicity data of compounds **1–5**.^a

Cell Line	Compound				
	1–2	3 ^a	4 ^a	5 ^a	5-FU ^a
HepG2(IC ₅₀)	-	297.97 ± 17.54	5.98 ± 0.12	9.97 ± 0.06	43.50 ± 3.69

^a Results are expressed as IC₅₀ values of mean \pm SD ($n = 3$) in μM .

Mangrove endophytic fungi have been proved to be particularly productive with regard to the accumulation of diverse biological natural products and yielded more than 800 natural products [16]. In our previous study, over 120 different compounds, with thirty of them being new polyketides, were discovered from mangrove endophytic fungi, including pyrones [17], isocoumarins [9,17], coumarins [18], cytosporones [18] and chromones [19], etc. In the current study, two new polyketides, cytospyrone (**1**), cytospomarin (**2**), together with three known metabolites (**3–5**) were isolated from the rice culture of *Cytospora* sp. from Chinese mangrove *Ceriops tagal*. Structurally, **1** and pestalotiopyrones A–H [17] are pyrone derivatives, having both a methoxy group positioned at C-4 and a substituted alkyl side chain at C-6, which all proved to be devoid of significant activity in the antimicrobial and

cytotoxic bioassays. Many naturally occurring isocoumarin and 3,4-dihydroisocoumarin derivatives are known to have substituents at C-3 and have been shown to possess an impressive array of biological activities [20]. Five dihydroisocoumarins isolated from *Cytospora eucalypticola* KC1636 [21] exhibited mildly antifungal and antibacterial activities towards Gram positive bacteria, which is similar to our biological finding on **2**. Compound **3** is closely related to 5-dehydroxycytosporone E previously reported from another *Cytospora* sp. TT-10, both featuring a phthalan-1-one skeleton [22]. Previously other fungal cytosporone derivatives that bear structural similarities to **3** isolated in our study had been described to be cytotoxic against several cancer cell lines in vitro [23], in contrast to the previous report, **3** showed no activity towards the bioassays we investigated. Integracins A (**4**) and B (**5**), exhibited potent (human immunodeficiency virus Type 1) HIV-1 integrase inhibitors, and were dimeric alkyl aromatic compounds isolated for the first time from *Cytonaema* sp. living in twigs of *Quercus ilex* [13]. They were later found to be produced by various organisms, such as endophytic fungi *Cytospora* sp. [22], Chinese mangrove plant *Sonneratia hainanensis* [24] and *Laguncularia racemose* [25]. Moreover, compound **4** was also reported to possess potent cytotoxicity against the tumor cell lines HepG2 and NCI-H460 with both 100% inhibitions at 25 mg/mL [24]. In this work, we found not only **4** but **5** strongly inhibited the proliferation of human cancer cell line HepG2, which was in accordance with previous reports. This highlighted the high potential of bioprospecting of polyketides from mangrove endophytic fungi *Cytospora*.

3. Materials and Methods

3.1. General Experimental Procedures

Optical rotations were measured on a WYA-2S digital Abbe refractometer (Shanghai Physico-optical Instrument Factory, Shanghai, China). UV spectra were obtained on a Shimadzu UV-2401 PC spectrophotometer (Shimadzu Corporation, Tokyo, Japan). Then, 1D and 2D NMR spectra were recorded on Bruker AV 400 NMR apparatus (Bruker Biospin Group, Karlsruhe, Germany) in CD₃OD, DMSO-*d*₆ or CDCl₃ (Guangzhou Chemical Reagent Factory, Guangzhou, China). Mass spectra were obtained on a LTQ Orbitrap XL instrument (Thermo Fisher Scientific, Bremen, Germany) using peak matching. Column chromatography was performed with silica gel (200–300 mesh, Qingdao Haiyang Chemical Co., Qingdao, China) and Sephadex LH-20 (18–110 μm, Merck, Darmstadt, Germany). Semi-preparative HPLC was achieved on an Agilent 1100.

3.2. Fungal Material and Identification

Following standard procedures [26], endophytic fungi were isolated from fresh, healthy hypocotyls of *Ceriops tagal* (Rhizophoraceae), which were collected in October 2015 in Dong Zhai Gang-Mangrove Garden on Hainan Island, China. The fungus (strain no. JGM-9) was identified as *Cytospora* sp. (GenBank accession no. MG948459) according to DNA amplification and sequencing of the internal transcribed spacer (ITS) region. A voucher strain was deposited at one of the authors' laboratory (J.X.).

3.3. Fermentation, Extraction and Isolation

The fungus was grown on solid rice medium at room temperature in 1000 mL-Erlenmeyer flasks containing 100 g rice (Jiangxi COFCO Rice Industry Co., Nanchang, China) and 100 mL-seawater. After 39 days of cultivation, the mycelia and solid rice medium were extracted with ethyl acetate (EtOAc). The extract was evaporated under reduced pressure to yield 90.0 g residue. This residue was subjected to silica gel column chromatography (CC) employing a step gradient of petroleum ether/ethyl-acetate gradient (100:0 to 0:100) to obtain four fractions (Fr. 1–Fr. 7). Promising Fr. 5 was separated by CC (silica gel; petroleum ether/ethyl acetate/acetone 5:2:2) to give four sub-fractions. Sub-Fr. 5–2 was purified with silica gel by CHCl₃/MeOH 20:1 and reversed-phase-HPLC (MeOH/H₂O 80:20) to yield compound **2** (15.0 mg). Sub-Fr. 5–3 was subjected to CC (Sephadex LH-20, MeOH/CHCl₃ 1:1) and reversed-phase-HPLC (MeOH/H₂O 70:30 to 100:0) to furnish **1** (8.1 mg), **4** (5.7 mg) and **5** (3.8 mg).

Fr. 7 was subjected to CC (silica gel; gradient petroleum ether / acetone) and reversed-phase-HPLC (MeOH/H₂O 80:20 to 100:0) to afford **3** (3.8 mg).

Cytospyrone (**1**): white amorphous powder (MeOH); $[\alpha]_D^{20} = -23.1^\circ$ (c 0.05, MeOH); UV (MeOH) λ_{\max} 212 nm; ¹H NMR (400 MHz, CD₃OD) δ_H 6.47 (1H, s, H-5), 5.32 (1H, d, $J = 9.1$ Hz, H-4'), 5.29 (1H, d, $J = 9.0$, 6'), 4.10 (1H, q, $J = 6.4$, H-8'), 4.08 (1H, d, $J = 9.6$, H-1'), 3.94 (3H, s, 4-OCH₃), 3.33–3.42 (1H, m, H-5'), 2.79 (1H, m, H-2'), 1.85 (3H, s, 3-CH₃), 1.67 (3H, s, 3'-CH₃), 1.65 (3H, s, 7'-CH₃), 1.18 (3H, d, $J = 6.4$, H-9'), 1.07 (3H, d, $J = 7.0$, 2'-CH₃), 1.03 (3H, d, $J = 6.7$, 5'-CH₃); ¹³C-NMR (100 MHz, CD₃OD) δ_C 169.1 (C-4), 168.5 (C-2), 167.8 (C-6), 138.1 (C-7'), 135.3 (C-4'), 134.2 (C-3'), 130.1 (C-6'), 101.5 (C-3), 97.5 (C-5), 80.7 (C-1'), 73.9 (C-8'), 57.3 (4-OCH₃), 44.1 (C-2'), 32.3 (C-5'), 21.9 (C-9'), 21.7 (5'-CH₃), 16.2 (3'-CH₃), 11.8 (7'-CH₃), 10.8 (3'-CH₃), 8.4 (3-CH₃); HR-ESI-MS m/z 373.1991 [M + Na]⁺ (calculated for C₂₀H₃₀O₅Na, 373.1991) (Supplementary Materials).

Cytospomarin (**2**): a yellow amorphous solid (MeOH); $[\alpha]_D^{20} = +11.7^\circ$ (c 0.3, MeOH); UV (MeOH) λ_{\max} 318 nm, 247 nm; ¹H NMR (400 MHz, DMSO-*d*₆) δ_H 10.8 (1H, br s, 6-OH), 6.53 (1H, s, H-4), 6.33 (1H, s, H-7), 3.92–4.00 (1H, m, H-10) 3.68 (3H, s, 5-OCH₃), 2.50–2.57 (2H, m, H-9), 1.12 (3H, d, $J = 6.2$, H-11); ¹³C-NMR (100 MHz, DMSO-*d*₆) δ_C 165.6 (C-1), 161.1 (C-8), 158.6 (C-6), 154.7 (C-3), 134.3 (C-5), 130.3 (C-5a), 102.6 (C-7), 99.9 (C-4), 95.5 (C-8a), 64.0 (C-10), 60.4 (5-OCH₃), 42.8 (C-9), 23.3 (C-11); HRESIMS m/z 289.0674 [M + Na]⁺ (calculated for C₁₃H₁₄O₆Na, 289.0610).

Dimethoxyphthalide (**3**): white amorphous powder (MeOH); $[\alpha]_D^{20} = +123^\circ$ (c 0.1, MeOH), UV (MeOH) λ_{\max} 216 nm, ¹H NMR (400 MHz, CDCl₃) δ_H 6.55 (1H, s, H-4), 5.40 (1H, d, $J = 6.6$, H-3), 4.05 (3H, s, 7-OCH₃), 3.92 (3H, s, 5-OCH₃), 2.14 (3H, s, 6-CH₃), 1.59 (3H, d, $J = 6.6$, 3-CH₃); ¹³C-NMR (100 MHz, CDCl₃) δ_C 168.3 (C-1), 164.2 (C-5), 157.6 (C-7), 152.9 (C-3a), 120.5 (C-6), 109.7 (C-7a), 97.9 (C-4), 76.4 (C-3), 62.1 (7-OCH₃), 56.1 (5-OCH₃), 29.7 (C-9), 20.7 (C-8); HRESIMS m/z 233.0969 [M + H]⁺ (calculated for C₁₂H₁₅O₄, 233.0969). The data of ¹H NMR and ¹³C NMR are basically consistent with those reported in literature [12].

Integracin A (**4**): yellow oil (MeOH); $[\alpha]_D^{20} = +97.0^\circ$ (c 0.1, MeOH); UV (MeOH) max 280, 259, 218 nm; ¹H NMR (500 MHz, CD₃OD) 6.23 (H, d, $J = 1.8$, H-6'), 6.19 (H, d, $J = 1.8$, H-4'), 6.14 (2H, d, $J = 1.4$, H-1, H-5), 6.10 (H, br s, H-3), 5.28 (H, pent, $J = 5.6$ Hz, H-14), 4.82 (H, overlapped, H-15'), 2.81–2.85 (2H, m, H-8'), 2.45 (H, t, $J = 8.0$ Hz, H-7), 2.03 (3H, s, Me-2''), 1.66–1.76 (4H, m, H-13, H-15), 1.54–1.57 (4H, m, H-8, H-9'), 1.40–1.42 (4H, m, H-14', H-16'), 1.31–1.35 (20H, m, 9-H to 12-H, H-16, H-10' to H-13', H-17'), 0.99 (3H, t, $J = 7.3$ Hz, Me-18'), 0.94 (3H, t, $J = 7.3$, Me-17); ¹³C-NMR (125 MHz, CD₃OD) δ 173.1 (C-1'), 172.7 (C-1''), 165.9 (C-3'), 163.5 (C-5'), 159.2 (C-2, C-4), 149.0 (C-7'), 146.3 (C-6), 111.9 (CH-6'), 107.9 (CH-1, CH-5), 105.8 (C-2'), 101.9 (CH-4'), 101.0 (CH-3), 76.7 (CH-14), 75.5 (CH-15'), 37.7 a (CH₂-8'), 37.4 a (CH₂-15), 37.4 a (CH₂-16'), 36.9 (CH₂-7), 35.2 (CH₂-13), 35.2 (CH₂-14'), 33.6 (CH₂-9'), 32.3 (CH₂-8), 31.0 a (CH₂-10'), 30.7 a (CH₂-11'), 30.5 a (CH₂-12'), 30.5 a (CH₂-11), 30.4 a (CH₂-10), 30.2 (CH₂-9), 26.6 (CH₂-13'), 26.4 (CH₂-12), 21.2 (CH₃-2''), 19.9 (CH₂-16), 19.6 (CH₂-17'), 14.3 (CH₃-18'), 14.2 (CH₃-17), chemical shifts could be interchanged; ESI-MS [M + H]⁺ m/z 629.4 (C₃₇H₅₇O₈). The data of ¹H NMR and ¹³C NMR are basically consistent with those reported in literature [13].

Integracin B (**5**): yellow oil (MeOH); $[\alpha]_D^{20} = +37.8^\circ$ (c 0.30, MeOH); UV (MeOH) λ_{\max} 300, 264, 230 nm; ¹H NMR (500 MHz, CD₃OD) δ 11.98 (H, s, 3'-OH), 7.61 (H, br s, 3×-OH), 6.21 (H, d, $J = 2.4$, H-6'), 6.19 (H, d, $J = 2.4$ Hz, H-4'), 6.14 (2H, d, $J = 2.1$, H-1, H-5), 6.10 (H, t, $J = 2.1$, H-3), 5.20 (H, pent, $J = 5.7$, H-14), 3.48–3.52 (H, m, H-15'), 2.80 (2H, td, $J = 7.0, 2.5$, H-8'), 2.40 (H, t, $J = 7.5$, H-7), 1.63–1.67 (2H, m, H-13), 1.59–1.63 (2H, m, H-15), 1.48–1.55 (4H, m, H-8, H-9'), 1.36–1.39 (4H, m, H-14', H-16'), 1.34–1.36 (2H, m, H-17'), 1.28–1.30 (2H, m, H-16), 1.23–1.28 (20H, m, 9-H to 12-H, H-16, H-10' to H-13', H-17'), 0.91 (3H, t, $J = 7.3$, Me-18'), 0.88 (3H, t, $J = 6.8$, Me-17); ¹³C-NMR (125 MHz, CD₃OD) δ 172.3 (C-1'), 165.5 (C-3'), 162.8 (C-5'), 158.4 (C-2, C-4), 149.1 (C-7'), 146.1 (C-6), 111.8 (CH-6'), 107.8 (CH-1, CH-5), 105.1 (C-2'), 101.6 (CH-4'), 100.6 (CH-3), 76.3 (CH-14), 71.9 (CH-15'), 40.0 (CH₂-16'), 37.9 (CH₂-8'), 37.6 (CH₂-15), 37.2 (CH₂-7), 36.6 (CH₂-13), 35.0 (CH₂-14'), 33.1 (CH₂-9'), 31.9 (CH₂-8), 30.7 a (CH₂-10'), 30.5 a (CH₂-11'), 30.4 a (CH₂-12'), 30.1 a (CH₂-11), 30.0 a (CH₂-10), 29.9 (CH₂-9), 26.4 (CH₂-13'), 26.2 (CH₂-12), 19.5 (CH₂-16), 19.4 (CH₂-17'), 14.4 (CH₃-18'), 14.3 (CH₃-17), a chemical

shifts could be interchanged; ESIMS [M + H]⁺ *m/z* 587.4 (C₃₅H₅₅O₇). The data of ¹H NMR and ¹³C NMR are basically consistent with those reported in literature [13].

3.4. ECD Calculations

Monte Carlo conformational searches were carried out by means of Spartan 14 software using Merck molecular force field (MMFF). The conformers with Boltzmann population of over 1% were chosen for ECD calculations, and then the conformers were initially optimized at B3LYP/6-31g level in gas. The theoretical calculation of ECD was conducted in MeOH using time dependent density functional theory (TDDFT) at the B3LYP/6-31+g (d, p) level for all conformers of compounds **1** and **2**. ECD spectra were generated using the program SpecDis 1.6 (University of Würzburg, Würzburg, Germany) and GraphPad Prism 5 (University of California, San Diego, CA, USA) from dipole-length rotational strengths by applying Gaussian band shapes with sigma = 0.3 eV.

3.5. Optical Rotation (OR) Calculations

Monte Carlo conformational searches were carried out by means of Spartan 10 software using Merck molecular force field (MMFF). The conformers with Boltzmann population of over 1% were chosen for OR calculations, and then the conformers were initially optimized at B3LYP/6-31+g (d, p) level in MeOH using the conductor-like polarizable continuum model (CPCM) polarizable conductor calculation model. The theoretical calculation of OR was conducted in MeOH using time dependent density functional theory (TDDFT) at the B3LYP/6-31+g (d, p) level for all conformers of compound **2**.

3.6. Antimicrobial Activity

The antimicrobial activity was determined against human pathogens *Escherichia coli* GIM1.201, methicillin-resistant *Staphylococcus aureus* GIM1.771 (MRSA), *Pseudomonas aeruginosa* GIM1.200, *Candida albicans* GIM2.169 and plant pathogenic fungi *Bacillus subtilis*, *Colletotrichum gloeosporioides* and *Magnaporthe oryzae* (Guangdong Microbial Culture Collection Center, China, CDMCC). The bacteria was cultured in Luria-Bertani (LB) medium (10 g of peptone, 15 g of sodium chloride, 3 g of yeast extract, and 1000 mL of distilled H₂O) at 37 °C (160 rpm) for 24 h, and the fungi was cultured in potato dextrose broth (PDB) medium (200 g of potatoes, 20 g of dextrose, and 1000 mL of distilled H₂O) at 28 °C (160 rpm) for 48 h. All isolated compounds were subjected to antimicrobial assays using a serial dilution technique, as previously described [26]. The minimum inhibitory concentration (MIC) was assigned to the lowest concentration that completely inhibited the growth of the indicator microorganisms. Ciprofloxacin (Guangzhou Lianghua Chemical Co., Ltd., 99.9%, Guangzhou, China) and amphotericin (American AMRESCO, 99.9%, Branded Products Group, Cochran, USA) were used as a positive control.

3.7. Cytotoxicity Assay

The human hepatoma cell (HepG2) cells (Cell Resource Center, Shanghai Institutes for Biological Sciences, Chinese Academy of Sciences) were grown in RPMI-1640 culture medium. Cytotoxicity against HepG2 cells was evaluated using the 3-(4,5-dimethylthiazol-2-yl)-2,5-diphenyltetrazolium bromide (MTT) (Sigma-Aldrich, Missouri, St. Louis, MO, USA) method, as described previously [8] and 5-Fluorouracil (5-FU) (Beijing Solarbio Science & Technology Co., Ltd., 99.8%) (Beijing, China) was used as the positive control.

4. Conclusions

In the present work, two new polyketides cytospyrone (**1**), cytospomarin (**2**) and three known metabolites (**3–5**) were obtained from the ethyl acetate extract of the fermented cultures of the fungus *Cytospora* sp., which was isolated from the Chinese mangrove *Ceriops tagal*. Compound **2** exhibited

weak inhibitory activity against *Escherichiacoli* GIM1.201 and compounds 4 and 5 displayed potent cytotoxicity against human cancer cell line HepG2.

Supplementary Materials: The following are available online, Figure S1. ¹H-NMR of cytospyrone (1); Figure S2. ¹³C-NMR of cytospyrone (1); Figure S3. DEPT of cytospyrone (1); Figure S4. ¹H-¹H COSY of cytospyrone (1); Figure S5. HMQC of cytospyrone (1); Figure S6. HMBC of cytospyrone (1); Figure S7. ROESY of cytospyrone (1); Figure S8. HR-ESI-MS of cytospyrone (1); Figure S9 CD spectrum of cytospyrone (1); Figure S10. ¹H-NMR of cytospomarin (2); Figure S11. ¹³C-NMR of cytospomarin (2); Figure S12. DEPT of cytospomarin (2); Figure S13. ¹H-¹H COSY of cytospomarin (2); Figure S14. HMQC of cytospomarin (2); Figure S15. HMBC of cytospomarin (2); Figure S16. ROESY of cytospomarin (2); Figure S17. HR-ESI-MS of cytospomarin (2); Figure S18. CD spectrum of cytospomarin (2). **Table S1.** Gibbs free energies^a and equilibrium populations^b of low-energy conformers of cytospyrone; Table S2. Cartesian coordinates for the low-energy reoptimized MMFF conformers of cytospyrone (1) at B3LYP/6-31G(d,p) level of theory in gas; **Table S3.** Gibbs free energies^a and equilibrium populations^b of low-energy conformers of cytospomarin (2); Table S4. Cartesian coordinates for the low-energy reoptimized MMFF conformers of cytospomarin (2) at B3LYP/6-31G(d,p) level of theory in gas; Table S5. Gibbs free energies^a and equilibrium populations^b of low-energy conformers of cytospomarin (2); Table S6. Cartesian coordinates for the low-energy reoptimized MMFF conformers of cytospomarin (2) at B3LYP/6-31+G(d,p) level of theory in CH₃OH.

Author Contributions: C.W. and Q.D. isolated the compounds. Q.D. carried out the large-scale fermentation and extraction. M.S. performed antimicrobial and cytotoxic activity evaluation. J.X. designed and supervised this research, structure elucidation and manuscript preparation. J.X. designed and supervised this research. The final revision of the manuscript was revised by all the authors. All authors have read and agreed to the published version of the manuscript.

Funding: This work was financially supported by the High-level Talents Programs of Hainan Province (2019RC006), National Natural Science Foundation of China (no. 81973229/81660584), Key Research and Development Program of Hainan Province (ZDYF2017099). Key Project of Education Department of Hainan Province (Hnky2019ZD-6) and the Key Lab of Tropical Pharmaceutical Herb Chemistry of Hainan Province Open Fund in Hainan Normal University (RDZH2019004) are gratefully acknowledged.

Conflicts of Interest: The authors declare no conflict of interest.

References

1. Ancheeva, E.; Daletos, G.; Proksch, P. Lead compounds from mangrove-associated microorganisms. *Mar. Drugs* **2018**, *16*, 319. [[CrossRef](#)] [[PubMed](#)]
2. Xu, J. Bioactive natural products derived from mangrove-associated microbes. *RSC Adv.* **2015**, *5*, 841–892. [[CrossRef](#)]
3. Xu, J. Biomolecules produced by mangrove-associated microbes. *Curr. Med. Chem.* **2011**, *18*, 5224–5266. [[CrossRef](#)] [[PubMed](#)]
4. Zhou, J.; Xu, J. Chemistry and biodiversity of *Rhizophora*-derived endophytic fungi. In *Mangrove Ecosystem Ecology and Function*; IntechOpen: London, UK, 2018; Volume 8, pp. 165–186.
5. Debbab, A.; Aly, A.H.; Proksch, P. Mangrove derived fungal endophytes—a chemical and biological perception. *Fungal Divers.* **2013**, *61*, 1–27. [[CrossRef](#)]
6. Deng, Q.; Yang, X.B.; Lv, X.B.; Xu, J. Biomolecules produced by mangrove *Ceriops tagal* endophytic fungi. *Chin. J. Antibiot.* **2018**, *43*, 635–643.
7. Xu, Z.Y.; Xiong, B.X.; Xu, J. Chemical investigation of secondary metabolites produced by mangrove endophytic fungus *Phyllosticta capitalensis*. *Nat. Prod. Res.* **2019**, 1–5. [[CrossRef](#)]
8. Zhou, J.; Li, G.; Deng, Q.; Zheng, D.Y.; Yang, X.B.; Xu, J. Cytotoxic constituents from the mangrove endophytic *Pestalotiopsis* sp. induce G(0)/G(1) cell cycle arrest and apoptosis in human cancer cells. *Nat. Prod. Res.* **2018**, *32*, 2968–2972. [[CrossRef](#)]
9. Xu, Z.Y.; Wu, X.; Li, G.; Feng, Z.; Xu, J. Pestalotiopsis B, a new isocoumarin derivative from the mangrove endophytic fungus *Pestalotiopsis* sp. HHL101. *Nat. Prod. Res.* **2019**, 1–6. [[CrossRef](#)]
10. Hemberger, Y.; Xu, J.; Wray, V.; Proksch, P.; Wu, J.; Bringmann, G. Pestalotiopsis A and B: Stereochemically challenging flexible sesquiterpene-cyclopaldic acid Hybrids from *Pestalotiopsis* sp. *Chem. Eur. J.* **2013**, *19*, 15556–15564. [[CrossRef](#)]

11. Deng, Q.; Li, G.; Sun, M.Y.; Yang, X.B.; Xu, J. A new antimicrobial sesquiterpene isolated from endophytic fungus *Cytospora* sp. from the Chinese mangrove plant *Ceriops tagal*. *Nat. Prod. Res.* **2018**, *34*, 1404–1408. [[CrossRef](#)]
12. Bradamante, S.; Barenghi, L.; Beretta, G.; Bonfa, M.; Rollini, M.; Manzoni, M. Production of lovastatin examined by an integrated approach based on chemometrics and DOSY-NMR. *Biotechnol. Bioeng.* **2002**, *80*, 589–593. [[CrossRef](#)] [[PubMed](#)]
13. Singh, S.B.; Zink, D.L.; Bills, G.F.; Pelaez, F.; Teran, A.; Collado, J.; Silverman, K.C.; Lingham, R.B.; Felock, P.; Hazuda, D.J. Discovery, structure and HIV-1 integrase inhibitory activities of integracins, novel dimeric alkyl aromatics from *Cytospora* sp. *Tetrahedron Lett.* **2002**, *43*, 1617–1620. [[CrossRef](#)]
14. Cai, R.L.; Wu, Y.N.; Chen, S.H.; Cui, H.; Liu, Z.M.; Li, C.Y.; She, Z.G. Penisocoumarins A–J: Isocoumarins from *Penicillium commune* QQF-3, an endophytic fungus of the mangrove plant *Kandelia candel*. *J. Nat. Prod.* **2018**, *81*, 1376–1383. [[CrossRef](#)] [[PubMed](#)]
15. Savi, D.C.; Shaaban, K.A.; Mitra, P.; Ponomareva, L.V.; Thorson, J.S.; Glienke, C.; Rohr, J. Secondary metabolites produced by the citrus phytopathogen *Phyllosticta citricarpa*. *J. Antibiot.* **2019**, *72*, 306–310. [[CrossRef](#)]
16. Xu, J. *Natural Products of Mangrove-Derived Microbes*; Science Press: Beijing, China, 2014; ISBN 97-7-03-041971-2.
17. Xu, J.; Aly, A.H.; Wray, V.; Proksch, P. Polyketide Derivatives of endophytic fungus *Pestalotiopsis* sp. isolated from the Chinese mangrove plant *Rhizophora mucronata*. *Tetra Lett.* **2011**, *52*, 21–25. [[CrossRef](#)]
18. Xu, J.; Kjer, J.; Sendker, J.; Wray, V.; Proksch, P. Cytosporones, coumarins, and an alkaloid from the endophytic fungus *Pestalotiopsis* sp. isolated from the Chinese mangrove plant *Rhizophora mucronata*. *Bioorg. Med. Chem.* **2009**, *17*, 7362–7367. [[CrossRef](#)]
19. Xu, J.; Kjer, J.; Sendker, J.; Wray, V.; Proksch, P. Chromones from the endophytic fungus *Pestalotiopsis* sp. isolated from the Chinese mangrove plant *Rhizophora mucronata*. *J. Nat. Prod.* **2009**, *72*, 662–665. [[CrossRef](#)]
20. Thongbai, B.; Surup, F.; Mohr, K.; Kuhnert, E.; Hyde, K.D.; Stadler, M. Gymnopalynes A and B, chloropropynylisocoumarin antibiotics from cultures of the basidiomycete *Gymnopus* sp. *J. Nat. Prod.* **2013**, *76*, 2141–2144. [[CrossRef](#)]
21. Tetsuo, K.; Nigel, C.V.; Paul, D.B.; Monique, S.J.S. Dihydroisocoumarins and a tetralone from *Cytospora eucalypticola*. *Phytochemistry* **2003**, *62*, 779–782.
22. Takano, T.; Koseki, T.; Koyama, H.; Shiono, Y. A new cytosporone derivative from the endophytic fungus *Cytospora* sp. *Nat. Prod. Commun.* **2014**, *9*, 973–975. [[CrossRef](#)]
23. Brady, S.F.; Wagenaar, M.M.; Singh, M.P.; Janso, J.E.; Clardy, J. The cytosporones, new octaketide antibiotics isolated from an endophytic fungus. *Org. Lett.* **2000**, *23*, 4043–4046. [[CrossRef](#)] [[PubMed](#)]
24. Liu, H.L.; Huang, X.Y.; Li, J.; Xin, G.R.; Guo, Y.W. Absolute configurations of integracins A, B, and 15'-dehydroxy-integracin B. *Chirality* **2012**, *24*, 459–462. [[CrossRef](#)] [[PubMed](#)]
25. Shi, C.; Xu, M.J.; Bayer, M.; Deng, Z.W.; Kubbutat, M.H.G.; Waejen, W.; Proksch, P.; Lin, W.H. Phenolic compounds and their anti-oxidative properties and protein kinase inhibition from Chinese mangrove plant *Laguncularia racemose*. *Phytochemistry* **2010**, *71*, 435–442. [[CrossRef](#)] [[PubMed](#)]
26. Zhou, J.; Diao, X.P.; Wang, T.; Chen, G.Y.; Lin, Q.; Yang, X.B.; Xu, J. Phylogenetic diversity and antioxidant activities of culturable fungal endophytes associated with the mangrove species *Rhizophora stylosa* and *R. mucronata* in the South China Sea. *PLoS ONE* **2018**, *13*, e0197359. [[CrossRef](#)]

Sample Availability: Samples of the compounds are not available from the authors.



© 2020 by the authors. Licensee MDPI, Basel, Switzerland. This article is an open access article distributed under the terms and conditions of the Creative Commons Attribution (CC BY) license (<http://creativecommons.org/licenses/by/4.0/>).